Proceedings of the 21st ICSMGE, Vienna, Austria, 14 – 19 June 2026. Pistrol, Adam & Schweiger (eds.)
Published by: ÖGG, Austrian Society for Geomechanics, Salzburg, Austria, ISBN 978-3-9503898-4-5
https://doi.org/10.53243/ICSMGE2026-1337

Geological Uncertainty and Its Consideration in Geotechnical Analysis by Means of the Finite Element Method

Johannes Leo, Franz Tschuchnigg
Institute of Soil Mechanics, Foundation Engineering and Computational Geotechnics, Graz University of Technology, Austria, leo@tugraz.at

Georg Erharter
Norwegian Geotechnical Institute, Oslo, Norway

ABSTRACT: Understanding how subsoil uncertainties influence geotechnical structure performance is essential for improving design robustness. Accordingly, this study introduces a general workflow that integrates geological uncertainty into numerical geotechnical analyses to evaluate the variability of selected geotechnical target features. Geological uncertainty is quantified by treating the location of geological layer interfaces as one-dimensional random functions and simulating their spatial variability using (un)conditional simulation methods. These simulated stratification realizations are then integrated in an automated modelling and evaluation framework using the finite element method for analysis. Applicability and capabilities of the presented approach are demonstrated by two case studies, adopted from literature. The first examines a slope stability problem, where the geological interface significantly influences both the factor of safety and the predicted type of failure mechanism. A single strutted deep excavation is also investigated with the focus on demonstrating how structural elements can be integrated into the framework. While the strut's normal force shows notable variability under working load conditions, the factor of safety exhibits more moderate sensitivity to geological interface fluctuations for the considered boundary value problem. Although (right now) the requirements for a full reliability-based design are not met, the approach offers valuable insight into the role of geological uncertainty in geotechnical design.

KEYWORDS: Geological uncertainty, Geotechnical design, Finite Element analysis, Layer boundary uncertainty

1 INTRODUCTION

Geotechnical structures are inherently in contact with the natural ground, such as deep foundations, or utilize ground material as a construction medium, as for embankments or tunnels. Consequently, the success of a geotechnical project fundamentally depends on the appropriate consideration of the natural ground geometry and properties (Phoon, et al., 2022).

However, when it comes to subsoil uncertainty two main sources are identified: geotechnical uncertainty (GTU) and geological uncertainty (GLU) (Baecher and Christian, 2003). GTU refers to the location-dependent variation of material properties, a principle introduced into geotechnical engineering analyses in the 1970s (Vanmarcke, 1977). In reliability-based design, the influence of GTU is well investigated and its incorporation into geotechnical analysis is frequently considered in research. GLU in contrast, describes the lack of knowledge regarding the spatial distribution of a soil type, also interpreted as the uncertainty in layer boundary detection which found less attention than GTU in the past (Phoon, et al., 2022). Recent studies have demonstrated significant impacts of GLU on geotechnical analysis (Varkey, Hicks and Vardon, 2023), questioning the assumption of triviality. The impact of GLU - ranging from the basic conceptual geological model (CGM) to uncertainty interpretation and propagation into geotechnical analysis - remains insufficiently investigated and understood, restricting efforts to assess design robustness and optimize site investigation campaigns.

This paper presents a general workflow for investigating the influence of GLU on geotechnical structures, using two representative boundary value problems from the literature. The study not only highlights the impact of GLU but also demonstrates how the insights gained can support the development of more robust designs and increase confidence through a sound assessment of system behaviour. To narrow the focus for this work, boundary conditions such as the groundwater table or groundwater flow are temporarily set aside. Furthermore, potential future applications are discussed, emphasizing that a holistic consideration of GLU and GTU is essential for achieving optimal geotechnical design solutions.

2 GEOLOGICAL UNCERTAINTY & FEM

In the case of a fully deterministic finite element analysis (FEA), the geometry of the subsurface structures is generally based on a conservative estimate of the soil stratification (van den Eijnden, et al., 2024). However, determining which stratification configuration truly represents a conservative estimate is even for moderately complex geological conditions challenging. This difficulty arises because (i) the chain of consequences, triggered by the stratification configuration, is hard to estimate by engineering judgement alone and (ii) it is likely dependent on the specific design objective. As a result, there is a need to incorporate GLU in FEA to evaluate its impact on the geotechnical problem at hand (Phoon, et al., 2022). The approach illustrated in Figure 1 tackles this need by combining explicit probabilistic modelling of geological interfaces (GI) (van den Eijnden, et al., 2024) with parametric finite element analysis (PFEA).

The proposed framework, shown in Figure 1, which is based on the guidelines of Baynes and Parry (2024), begins with a desk study. Purpose of this phase is to gather existing documents and data of the project area. Based on the geological knowledge gained from these resources, a CGM is developed. The CGM provides an initial representation of the geological processes involved which are deemed to be critical for the geotechnical analysis, based on engineering judgement. For the stochastic stratigraphy simulation, discussed in more detail in 2.1, the CGM is further refined by data from site investigation campaigns (Phoon, Ching and Shuku, 2022). If site investigation data is not yet available at a particular project stage, a fully unconditional simulation can be performed using estimated GI variability. GLU accordingly can be assessed from the stochastic simulation (Wellmann and Regenauer-Lieb, 2012), however, this aspect is not discussed in the present work. In the next step, a PFEA is conducted for each GI realization. This process represents a Monte Carlo simulation of GI within a random finite element method analogy (Fenton and Griffiths, 2008), as described in 2.2.

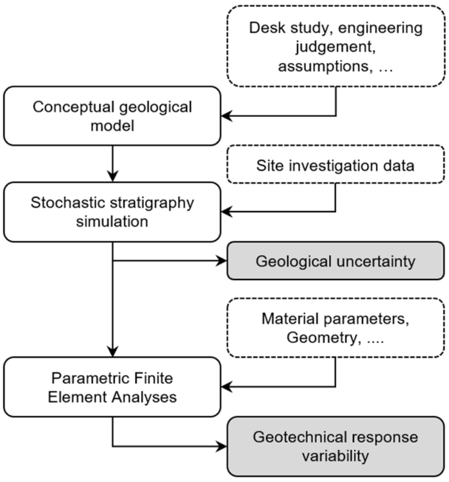

Figure 1. Workflow to assess the geotechnical response variability with respect to GLU.

2.1 *Geological interface variability*

GI variability is considered by an explicit boundary-based model (Xiao, et al., 2017) in this contribution, where the GI is treated as a one-dimensional random function (Baecher and Christian, 2003; Chiles and Delfiner, 2012). This approach is considered reasonable, as the investigated scenarios involve relatively simple, two-layered geological conditions with an assumed continuous GI across the entire model domain. If more complex geological conditions are described by the CGM a more sophisticated boundary-based approach or even a category-based geological model (Xiao, et al., 2017) needs to be considered.

Since the influence of site investigation design is not enclosed in this study, GI variability is considered by an unconditional simulation approach. The realizations are generated with the geostatistical Python library GSTools (Müller, et al., 2022) employing a Gaussian covariance model. Consequently, the GI is a function of the mean (μ), standard deviation (σ) and horizontal scale of fluctuation (δ_h), where δ_h is defined as twice the length scale of the covariance model used in GSTools (Vanmarcke, 1977) and σ is expressed by the coefficient of variation (COV). The COV is defined as shown in Equation (1). While these statistical parameters should ideally be derived from ground investigations in real projects (Phoon and Kulhawy, 1999; Lloret-Cabot, Fenton and Hicks, 2014), they are assumed here based on magnitudes reported in the literature (Phoon and Kulhawy, 1999; Cami, et al., 2020; Phoon, et al., 2022).

$$COV = {}^{\sigma}/_{\mu} \tag{1}$$

2.2 *Uncertainty propagation*

To investigate the influence of GI variability on geotechnical target parameters, e.g., factor of safety (FOS) or maximum anchor normal force, the GLU must be propagated through a translator, which is in this case a PFEA. This framework is widely known by the name RFEM, introduced by Fenton and Griffiths (2008) to incorporate GTU into geotechnical reliability analysis (Baecher and Christian, 2003).

As this study focuses on the influence of GLU, rather than GTU (Phoon, et al., 2022), the subsurface geometry is modeled stochastically as described in 2.1. Therefore, each random finite element model features a unique geometric configuration. To accommodate this, a fully automated model generation process is implemented in Plaxis 2D (Bentley Systems, 2024) utilizing its Python API, enabling a PFEA for each geological realization. The postprocessing step is also automated, allowing for the extraction of predefined geotechnical target parameters tailored for the boundary value problem under investigation. However, if the geotechnical target parameter must be evaluated over the whole domain, e.g., field stresses or strains, an additional postprocessing step is required. This involves interpolating the extracted field results from non-unique mesh configurations onto a regular grid to allow for the interpretation of the ensemble results. Finally, the geotechnical response variability is assessed by analyzing the ensemble of PFEA results for the pre-selected geotechnical target features.

3 EXAMPLE: SLOPE STABILITY ANALYSIS

The first example addresses a slope stability problem adopted from Griffiths and Lane (1999), in which the FOS and the critical failure mechanism of the slope is mainly conditional upon the ratio of the undrained shear strength (c_u) of the upper (c_{u1}) and lower (c_{u2}) layer (Guo and Griffiths, 2020). This sensitivity is also demonstrated in Schweiger (2005), who showed that performing a safety analysis using the strength reduction method within a FEA yields both the appropriate failure mechanism and the corresponding FOS. The dimensions of the deterministic base model used in this study are shown in Figure 2. It should be noted that the model length on the toe side of the slope has been extended by 20 m compared to the dimensions reported by Schweiger (2005) and Griffiths and Lane (1999).

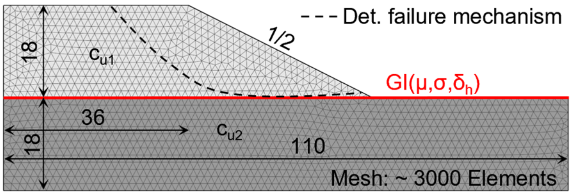

Figure 2. Model configuration slope stability example. The geological interface (GI) that is varied in the probabilistic analysis is highlighted in red.

The deterministic soil parameters for the linear elastic - perfectly plastic material model (for undrained conditions) are listed in Table 1. For the lower layer, a strength ratio of 1.6 relative to the upper layer is assumed. The model domain is discretized using approximately 3,000 elements with a fourth-order shape function, for every PFEA. The calculation sequence consists of three stages: an initialization stage using a gravity loading procedure, followed by a nil-step to rebalance the model and a safety phase that applies the strength reduction method to determine the FOS. A detailed description of the strength reduction method is found in Tschuchnigg, et al. (2015) or Tschuchnigg (2019).

Table 1. Soil parameters slope stability example.

Parameter	Symbol	Value	Unit
Unit weight	γ	20	kN/m^3
Young's modulus	E	10	MN/m^2
Poisson's ratio	ν	0.3	-
Undrained shear strength	c_{u1}	60	kPa
Strength ratio	c_{u2}/c_{u1}	1.6	-

From a stochastic point of view, the GI between the two layers, indicated by a red line in Figure 2, was modeled with a mean location (μ_{GI}) = 18 m, a COV_{GI} = 0.08 and a $\delta_{h,GI}$ = 40 m. The one-dimensional random function was sampled at a spatial resolution of 0.5 m and a total of 200 calculations were carried out to analyze the resulting geotechnical response variability.

3.1 *Variability of geotechnical features*

The sensitivity of the geotechnical slope stability analysis to GI variability is investigated based on the resulting variability in the FOS and the corresponding critical failure mechanism detected. Using fully deterministic input parameters, as presented in Figure 2 and Table 1, the safety analysis yields a FOS = 1.35, with the critical failure mechanism developing entirely within the upper soil layer (Schweiger, 2005; Guo and Griffiths, 2020). Further details on the influence of certain boundary conditions and strength ratios for the investigated boundary value problem can be found in Guo and Griffiths (2020).

However, the histogram of the FOS results from the analysis considering GI variability, shown in Figure 3, highlights its influence on the geotechnical analysis. It is evident that the GI has a substantial impact on the FOS of the slope, indicating that the strength ratio is not the only decisive factor. When a Gaussian probability density function is fitted to the data, a $\mu_{FOS} = 1.34$ and a $\sigma_{FOS} = 0.08$ are obtained. This results in a notable $COV_{FOS} = 0.06$ for the given boundary value problem. Additionally, the variability of the FOS is illustrated, in Figure 3 by the 95% confidence interval, indicated by red dashed lines.

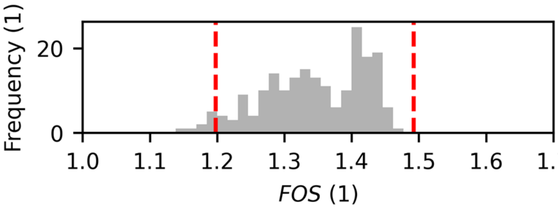

Figure 3. Results for FOS of the stochastic slope stability analysis, 95% confidence interval is indicated by red, dashed lines.

A second geotechnical target feature investigated is the delta incremental shear strain ($\Delta\gamma_s$) extracted over the entire model domain. This feature was selected because it aids in interpreting the present failure mechanism. However, the magnitude of $\Delta\gamma_s$ between individual PFEA is not directly comparable, hence, a min-max normalization is applied to the $\Delta\gamma_s$ field results in each realization. As a result, the normalized delta incremental shear strains ($\Delta\gamma_{s,norm}$) lie within the interval [0,1], allowing for an ensemble-based comparison across realizations.

The results for all realizations are shown in Figure 4, where the ensemble mean of the normalized delta incremental shear strains ($\mu_{\Delta\gamma s,norm}$) is plotted. As visible from the plot, and in contrast to the deterministic analysis, the critical failure mechanism does not consistently develop purely in the upper layer. Instead in some realizations the critical mechanism is formed through the base layer.

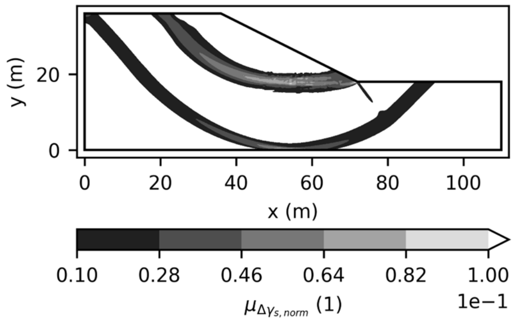

Figure 4. Mean of the normalized delta incremental shear strains ($\mu_{\Delta\gamma s,norm}$) for failure mechanism detection of the ensemble.

4 EXAMPLE: SINGLE STRUTTED EXCAVATION

The second synthetic case study used to analyze the influence of GI variability on geotechnical target parameters is a single strutted deep excavation problem. This boundary value problem was selected to contrast with the first example by introducing geotechnical structural elements such as a sheet pile wall and a strut and to highlight the variety of geotechnical target features that can be defined for analysis.

Geometric boundary conditions for the excavation are adopted from Schweiger (2005), respectively from Daxer, Tschuchnigg and Schweiger (2023) and are depicted in Figure 5. The total excavation depth is 8.0 m and the strut is situated 1.0 m below the initial ground level. The excavation is supported by a sheet pile wall, which is embedded 4.0 m measured from the bottom of the excavation. Unlike the boundary value problem reported in Schweiger (2005) and Daxer, Tschuchnigg and Schweiger (2023) the present study assumes two homogeneous soil layers, with a GI expected to lie at the maximum excavation depth.

The mesh configuration includes a refinement zone around the excavation and is designed to reach approximately a total of 3,300 elements for each PFEA. Consistent with the slope stability analysis, triangular elements with a fourth-order shape function are used. A representative mesh discretization of the model is included in Figure 5.

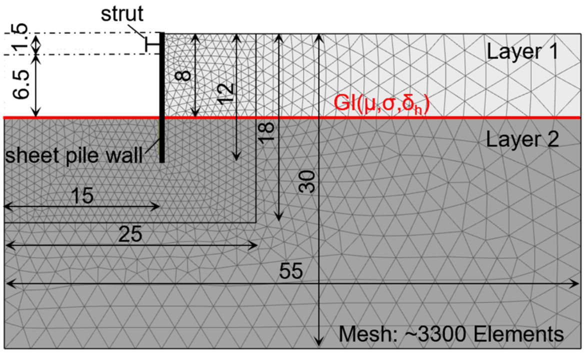

Figure 5. Model configuration single strutted excavation example. The geological interface (GI) that is varied in the probabilistic analysis is highlighted in red.

All structural elements are modelled by assuming linear – elastic material behavior and the corresponding parameters, adopted from Daxer, Tschuchnigg and Schweiger (2023) for the sheet pile wall and the strut are delineated in Table 2 and in Table 3 respectively. For both soil layers, the Hardening Soil (HS) model (Schanz, Vermeer and Bonnier, 1999) is used and the corresponding layer parameters considered in the analysis are listed in Table 4 and are adopted from Jürgens and Henke (2024).

Table 2. Parameters for the sheet pile wall.

Parameter	Symbol	Value	Unit
Normal stiffness	*EA*	3 008 000	kN/m
Bending stiffness	*EI*	68 400	kNm²/m
Prevent punching	-	No	

Table 3. Parameters for the strut.

Parameter	Symbol	Value	Unit
Normal stiffness	*EA*	7 200 000	kN
Spacing	*L*	1.0	m

Table 4. Soil parameters for the HS material model.

Parameter	Symbol	Layer 1	Layer 2	Unit
(Un-)saturated unit weight	γ_{unsat}, γ_{sat}	15	18	kN/m^3
Effective friction angle	φ'	25	30	°
Effective cohesion	c'	10	0	kPa
Dilatancy angle	ψ	0	0	°
Secant reference stiffness	E_{50}^{ref}	3.5	20	MPa
Oedometric reference stiffness	E_{oed}^{ref}	3.0	20	MPa
Un/reloading reference stiffness	E_{ur}^{ref}	7.0	60	MPa
Poisson's ratio un/reloading	ν_{ur}	0.2	0.2	-
Stress dependency index	m	0.9	0.5	-
Reference pressure	p_{ref}	100	100	kPa
Strength reduction factor	R_{inter}	0.64	0.63	-

The HS model belongs to the family of double hardening elastic-plastic material models, characterized primarily by a stress-dependent stiffness definition and the distinction between primary and secondary loading conditions. It should be noted, that in case of a safety analysis the HS model effectively reduces to a Mohr-Coulomb material model.

All structural elements are modeled assuming linear-elastic material behavior, with material parameters taken from Schweiger (2005). The soil-structure interaction between the sheet pile wall and the surrounding soil is considered using zero-thickness interface elements, applying the strength and stiffness parameters from the adjacent soil in combination with the strength reduction factor (R_{inter}) for the interface parameter determination. The related R_{inter} factors are provided in Table 4.

The GI variability, again indicated by a red line in Figure 5, is assumed by a mean depth (μ_{GI}) = 8 m, a $COV_{GI} = 0.1$ and a $\delta_{h,GI} = 30$ m. A sample resolution of the random function of 0.5 m was used and 200 realizations created.

The construction stages of the excavation are recreated in the numerical analysis by the following calculation phases:

- Phase 0: Initialization using the gravity loading procedure (non-horizontal layer boundary)
- Phase 1: Installation of sheet pile wall (wished-in-place) and excavation to a depth of 1.5 m
- Phase 2: Installation of the strut and excavation to a depth of 8 m
- Phase 3: Safety analysis employing the strength reduction method

4.1.1 *Variability of geotechnical features*

Geotechnical target features for the single strutted excavation were selected to investigate the influence of the GI variability on both the deformation behavior and maximum structural forces under working load conditions and the overall stability of the excavation (Daxer, Schweiger and Tschuchnigg, 2022). It should be noted, however, that characteristic input values for the soil parameters are used and the structures are considered to behave linear elastic. Furthermost, the analysis does not aim to fulfill the requirements of a reliability-based design (Baecher and Christian, 2003; van den Eijnden, et al., 2024), but rather serves to illustrate the variability of key geotechnical target features.

To gain insights on the behaviour under working load conditions, two different geotechnical target features are defined. Results are extracted at the end of Phase 2, i.e., after the excavation reached its final state. The first target feature is the normal force in the strut. Corresponding results of the ensemble are illustrated by a histogram plot in Figure 6. The struts normal force exhibits notable variability and when a Gaussian probability density function is fitted to the data, a $COV_F = 0.09$ is obtained. For reference, the fully deterministic analysis predicted a strut normal force F = -103 kN, while the upper bound of the 95% confidence interval, highlighted by red dashed lines in Figure 6, lies approximately at -140 kN.

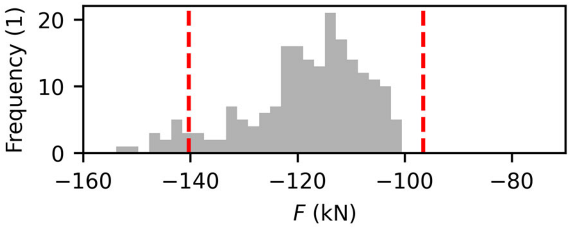

Figure 6. Histogram of strut normal force (F) results including the 95% confidence interval shown by red dashed lines.

Secondly, the deformation behavior of the sheet pile wall is used as a geotechnical target feature. Compared to the approach described in 3.1 for the field results, the complexity of the comparison is reduced, as no normalization is required. Anyway, interpolation onto a regular grid is still necessary. Figure 7 presents the distribution of the mean horizontal deflection of the sheet pile wall ($\mu_{ux,wall}$), as derived from the ensemble results. The estimated variability is also shown by the 95% confidence interval, assuming a Gaussian probability density function. Based on these results it is valid to conclude, that also the deformation behavior of the sheet pile wall exhibits a noteworthy degree of variability, highlighting the significant influence of GI variability even for a relatively simple excavation and stratification scenario. Interestingly, the deterministic results based on a perfectly horizontal GI ($u_{x,wall}$) is underestimated by $\mu_{ux,wall}$, in this particular case study.

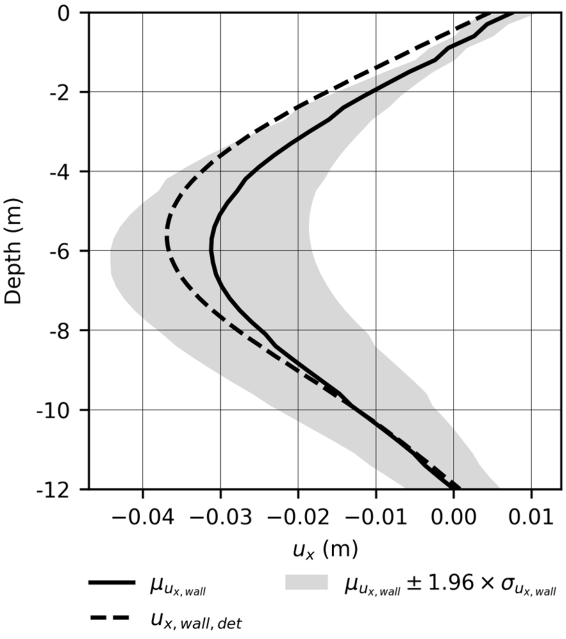

Figure 7. Horizontal deflection of sheet pile wall after final excavation.

The variability of the overall stability of the excavation is expressed by the FOS, which is determined by the strength reduction method. Results for this analysis are extracted from

Phase 3, which represents the safety analysis stage in the numerical model. For the excavation's FOS, a $COV_{FOS} = 0.02$ is determined. This lower degree of variability is also visible in the relatively narrow spacing of the upper and lower limit of the 95% confidence interval, indicated by red dashed lines in Figure 8. The fully deterministic analysis yields a FOS = 1.84, which is in good agreement with the mean of the ensemble results. To give a benchmark for analysis effort invested, the computation time for the 200 PFEA conducted for this case study was approximately 7 hours, which can be easily executed overnight.

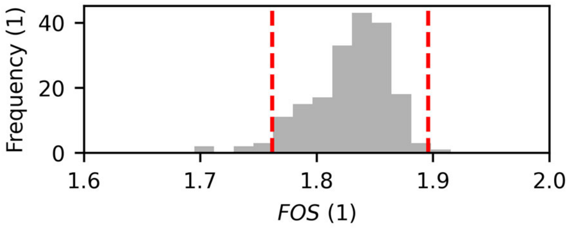

Figure 8. Histogram of factor of safety (FOS) results including the 95% confidence interval shown by red, dashed lines.

5 CONCLUSIONS

This contribution presents a workflow designed to investigate the influence of GLU, specifically the variability of GI, on selected geotechnical target features. The approach builds upon a CGM, which is extended by using information from site investigations to perform explicit stochastic simulations of the GI via (un-)conditional simulation methods. The GI, treated as a one-dimensional random function, is integrated into a fully automated framework that combines Plaxis 2D with its Python API. Enabling the stochastic simulation of the GI, the generation and computation of the boundary value problems and the extraction of geotechnical target features, effectively implementing a random finite element method approach. The resulting GI variability is translated into geotechnical variability by the numerical model and is assessed through ensemble-based interpretation of pre-selected target features.

The first synthetic case study presented, focused on a slope stability problem. It investigated how the spatial location of the GI separating two homogeneous soil layers affects both the FOS and the critical failure mechanism formed. The results showed that the distribution of the GI has a significant influence on the FOS and its corresponding variability. Normalized shear strain fields were used to visualize and interpret the ensemble-based distribution of failure patterns, revealing a high degree of variability in failure mechanisms.

A single strutted deep excavation was considered in the second synthetic case study. Here, the focus was on showcasing the flexibility of the proposed workflow by incorporating structural elements and evaluating the behavior under working load conditions and the overall stability of the excavation. The deformation behavior and the internal forces under working load conditions were analyzed by the sheet pile wall deflection and the strut normal force respectively. While the strut normal forces and the sheet pile wall deformations exhibited notable variability due to GLU. Even tough, the GLU provoked only limited variability in FOS, this case study underscores the importance of incorporating GLU, even in relatively simple stratification scenarios. Not only is the deformation behavior of the sheet pile affected, but also the bending moments will exhibit significant fluctuations due to GLU. Furthermore, future analyses should consider variations in the groundwater table, as these are expected to have a substantial influence on the structural response.

While this study has its emphasis on the influence of GLU on geotechnical target features variability, the approach does not aim to fulfill the requirements of a reliability-based design for the time being. Rather, it provides a clear illustration of how GI variability can influence geotechnical analyses. However, compared to conventional deterministic analyses, the proposed approach offers significantly richer insights into the behavior of geotechnical structures, while requiring only limited additional human effort due to its fully automated workflow. Although the interpretation of site investigation data must include an estimation of GI variability, the effort invested at this early stage yields substantial benefits in the quality and depth of the resulting analysis.

Future work should include the combined incorporation of GTU and GLU as neither cancels out the other. Applying the workflow to real-world projects at different design stages will help validate and extend its utility. Additionally, future research will address cause-and-effect relationships related to extreme scenarios to enhance both the understanding of geotechnical system behavior and the related design robustness.

6 ACKNOWLEDGEMENTS

This research was conducted as part of the "Ground and Soil Improvement modelling" project, funded by the Austrian Research Promotion Agency (FFG).

7 REFERENCES

Baecher, G. B. and Christian, J. T., 2003. *Reliability and statistics in geotechnical engineering. [e-book]:* John Wiley & Sons Ltd. <https://permalink.obvsg.at/>.

Baynes, F. and Parry, S., 2024. *Guidelines for the development and application of engineering geological models on projects.* 2nd ed. <https://www.iaeg.info/C25EGMGuidelines/>.

Bentley Systems, 2024. *Reference Manual 2D: Plaxis 2D 2024.1.*

Cami, B., Javankhoshdel, S., Phoon, K.-K. and Ching, J., 2020. Scale of Fluctuation for Spatially Varying Soils: Estimation Methods and Values. *ASCE-ASME Journal of Risk and Uncertainty in Engineering Systems, Part A: Civil Engineering,* [e-journal] 6(4). http://dx.doi.org/10.1061/AJRUA6.0001083.

Chiles, J.-P. and Delfner, P., 2012. *Geostatistics: Modeling spatial uncertainty.* 2nd ed. Oxford: Wiley-Blackwell.

Daxer, H.-P., Schweiger, H. F. and Tschuchnigg, F., 2022. Ultimate limit state design of deep excavation problems according to EC7 using numerical methods. *ISSMGE.* http://dx.doi.org/10.53243/NUMGE2023-105.

Daxer, H.-P., Tschuchnigg, F. and Schweiger, H. F., 2023. Ultimate limit state design for deep excavations according to Eurocode 7 by means of numerical methods. In: Romanian Society for Soil Mechanics and Geotechnical Engineering (SRGF), ed. 2023. *Proceedings of the 17th Danube - European Conference on Geotechnical Engineering.* Bucharest, Romania, pp. 185–192.

Fenton, G. A. and Griffiths, D. V., 2008. *Risk Assessment in Geotechnical Engineering:* Wiley.

Griffiths, D. V. and Lane, P. A., 1999. Slope stability analysis by finite elements. *Géotechnique,* [e-journal] 49(3), pp. 387–403. http://dx.doi.org/10.1680/geot.1999.49.3.387.

Guo, S. and Griffiths, D. V., 2020. Failure mechanisms in two-layer undrained slopes. *Canadian Geotechnical Journal,* [e-journal] 57(10), pp. 1617–1621. http://dx.doi.org/10.1139/cgj-2019-0642.

Jürgens, H. and Henke, S., 2024. Numerical Optimisation of Excavation Pit Design Using Finite Element Analyses. *Geotechnical and Geological Engineering,* [e-journal] 42(3), pp. 1659–1673. http://dx.doi.org/10.1007/s10706-023-02639-7.

Lloret-Cabot, M., Fenton, G. A. and Hicks, M. A., 2014. On the estimation of scale of fluctuation in geostatistics. *Georisk: Assessment and Management of Risk for Engineered Systems and Geohazards,* [e-journal] 8(2), pp. 129–140. http://dx.doi.org/10.1080/17499518.2013.871189.

Müller, S., Schüler, L., Zech, A. and Heße, F., 2022. GSTools v1.3: a toolbox for geostatistical modelling in Python. *Geoscientific Model Development,* [e-journal] 15(7), pp. 3161–3182. http://dx.doi.org/10.5194/gmd-15-3161-2022.

Phoon, K.-K., Cao, Z.-J., Ji, J., Leung, Y. F., Najjar, S., Shuku, T., Tang, C., Yin, Z.-Y., Ikumasa, Y. and Ching, J., 2022. Geotechnical uncertainty, modeling, and decision making. *Soils and Foundations,* [e-journal] 62(5), p. 101189–101189. http://dx.doi.org/10.1016/j.sandf.2022.101189.

Phoon, K.-K., Ching, J. and Shuku, T., 2022. Challenges in data-driven site characterization. *Georisk: Assessment and Management of Risk for Engineered Systems and Geohazards,* [e-journal] 16(1), pp. 114–126. http://dx.doi.org/10.1080/17499518.2021.1896005.

Phoon, K.-K. and Kulhawy, F. H., 1999. Characterization of geotechnical variability. *Canadian Geotechnical Journal,* [e-journal] 36(4), pp. 612–624. http://dx.doi.org/10.1139/t99-038.

Schanz, T., Vermeer, P. A. and Bonnier, P. G., 1999. The hardening soil model: Formulation and verification. In: R. B. J. Brinkgreve, ed. 1999. *Beyond 2000 in computational geotechnics: 10 years of PLAXIS International / edited by Ronald B.J. Brinkgreve.* Rotterdam: Balkema.

Schweiger, H. F., 2005. Application of FEM to ULS design (Eurocodes) in surface and near surface geotechnical structures. In: 2005. *11th International Conference on Computer Methods and Advances in Geomechanics: IACMAG.* Turin. Italien, pp. 419–430.

Tschuchnigg, F., 2019. *A Contribution to Computational Geotechnics - Theory and Practice.* Habilitation. Graz University of Technology.

Tschuchnigg, F., Schweiger, H. F., Sloan, S. W., Lyamin, A. V. and Raissakis, I., 2015. Comparison of finite-element limit analysis and strength reduction techniques. *Géotechnique,* [e-journal] 65(4), pp. 249–257. http://dx.doi.org/10.1680/geot.14.P.022.

van den Eijnden, B., Knuuti, M., Lesny, K., Löfman, M., Mavritsakis, A., Roubos, A., Schweckendiek, T., Sciarretta, F., Ebener, A., Escher, K., Spross, J., Commend, S., Hehenkamp, M., Arnold, P., Wilhelm, S., Ene, A., Rimoldi, P. and Pereira, R., 2024. *Reliability-based verification of limit states for geotechnical structures: Guidelines for the application of the 2nd generation of Eurocode 7: geotechnical design.* Luxembourg: Publications Office of the European Union.

Vanmarcke, E. H., 1977. Probabilistic Modeling of Soil Profiles. *Journal of the Geotechnical Engineering Division,* [e-journal] 103(11), pp. 1227–1246. http://dx.doi.org/10.1061/AJGEB6.0000517.

Varkey, D., Hicks, M. A. and Vardon, P. J., 2023. Effect of uncertainties in geometry, inter-layer boundary and shear strength properties on the probabilistic stability of a 3D embankment slope. *Georisk: Assessment and Management of Risk for Engineered Systems and Geohazards,* [e-journal] 17(2), pp. 262–276. http://dx.doi.org/10.1080/17499518.2022.2101066.

Wellmann, F. and Regenauer-Lieb, K., 2012. Uncertainties have a meaning: Information entropy as a quality measure for 3-D geological models. *Tectonophysics,* [e-journal] 526-529, pp. 207–216. http://dx.doi.org/10.1016/j.tecto.2011.05.001.

Xiao, T., Zhang, L.-M., Li, X.-Y. and Li, D.-Q., 2017. Probabilistic Stratification Modeling in Geotechnical Site Characterization. *ASCE-ASME Journal of Risk and Uncertainty in Engineering Systems, Part A: Civil Engineering,* [e-journal] 3(4). http://dx.doi.org/10.1061/AJRUA6.0000924.